cape3

Mesoscale Simulations of a Florida Sea Breeze Using the PLACE Land Surface Model Coupled to a 1.5-Order Turbulence Parameterization

Barry H. Lynn, etc.

The simulation of spring and summertime thunderstorms, sea-breezes, lake breezes, etc requires robust, forecast simulations of the atmospheric planetary boundary layer (PBL), as well as vertical transports of heat and moisture from the top of the PBL into the clouds above. Both depend quite strongly on the underlying characteristics of the land surface. The land surface affects the processing of solar energy: drier or more sparsely vegetated land surfaces produce more heat than water bodies or wetter or more heavily vegetated land surfaces. At the same time, wetter land surfaces produce more moisture than drier land surfaces. Thus, it might be very hot above a parking lot, but relatively cool and damp above a swamp.

To improve weather prediction of thunderstorms, etc, a sophisticated land-surface model, PLACE, the Parameterization for Land Atmospheric Convective Exchange, has been has been linked to a PBL model that calculates the transfer of heat and moisture witin it using the "turbulence kinetic energy." Both models have been incorporated into the Penn State/National Center for Atmospheric Research (PSU/NCAR) mesoscale model MM5.

A validation study used the newly developed model to simulate the evolution of Florida sea-breeze thunderstorms during the Convection and Precipitation Electrification Experiment (CaPE). Overall, eight simulations tested the sensitivity of the MM5 model to combinations of the new and default model physics, including soil moisture and temperature derived from off-line simulations of the PLACE model. Our study showed the importance of each model improvement in making a simulation that agreed most with observations. Most importantly, the new model better predicted the timing and location of thunderstorms than the original MM5 model.

The new model should provide the weather forecaster and climate scientist with better tools to predict thunderstorm development and other weather systems that occur during the spring and summer months, such as severe weather outbreaks, monsoons, and hurricanes.

cape3

Mesoscale Simulations of a Florida Sea Breeze Using the PLACE Land Surface Model Coupled to a 1.5-Order Turbulence Parameterization

Barry H. Lynn[1], David R. Stauffer[2], Peter J. Wetzel[3], Wei-Kuo Tao[3], Pinhas Alpert[4], Nataly Perlin[4], R. David Baker[5], Ricardo Munoz[2], Aaron Boone[6], and Yiqin Jia[6]

[1]Columbia University Center for Climate Systems Research
New York, New York, USA
and
NASA Goddard Space Flight Center
Mesoscale Atmospheric Processes Branch
Greenbelt, Maryland, USA

[2]The Pennsylvania State University
Department of Meteorology
University Park, Pennsylvania, USA

[3]NASA Goddard Space Flight Center
Mesoscale Atmospheric Processes Branch
Greenbelt, Maryland, USA

[4]Department of Geophysics and Planetary Sciences
Tel Aviv University
Tel Aviv
Israel

[5]Universities Space Research Association
NASA Goddard Space Flight Center
Mesoscale Atmospheric Processes Branch
Greenbelt, Maryland, USA

[6]Science Systems and Applications Incorporated
NASA Goddard Space Flight Center
Greenbelt Maryland, USA

Submitted to

Monthly Weather Review

September 3, 1999

Address for correspondence: Dr. Barry Lynn, NASA Goddard Space Flight Center, Mesoscale Atmospheric Processes Branch, Building 33, Code 912, Greenbelt, MD 20771. e-mail: lynn@agnes.gsfc.nasa.gov

Abstract

A sophisticated land-surface model, PLACE, the Parameterization for Land Atmospheric Convective Exchange, has been coupled to a 1.5-order turbulent kinetic energy (TKE) turbulence sub-model. Both have been incorporated into the Penn State/National Center for Atmospheric Research (PSU/NCAR) mesoscale model MM5. Such model improvements should have their greatest effect in conditions where surface contrasts dominate over dynamic processes, such as the simulation of warm-season, convective events. A validation study used the newly coupled model, MM5 TKE-PLACE, to simulate the evolution of Florida sea-breeze moist convection during the Convection and Precipitation Electrification Experiment (CaPE). Overall, eight simulations tested the sensitivity of the MM5 model to combinations of the new and default model physics, and initialization of soil moisture and temperature. The TKE-PLACE model produced more realistic surface sensible heat flux, lower biases for surface variables, more realistic rainfall, and cloud cover than the default model. Of the 8 simulations with different factors (*i.e.*, model physics or initialization), TKE-PLACE compared very well when each simulation was ranked interms of biases of the surface variables and rainfall, and percent and root mean square of cloud cover. A factor separation analysis showed that a successful simulation required the inclusion of a multi-layered, land surface soil vegetation model, realistic initial soil moisture, and higher order closure of the planetary boundary layer (PBL). These were needed to realistically model the effect of individual, joint, and synergistic contributions from the land surface and PBL on the CaPE sea-breeze, Lake Okeechobee lake breeze, and moist convection.

1 Introduction

The evolution of the Florida sea-breeze has been studied by numerous researchers (*e.g.*, Byers and Rosebush, 1948; Pielke, 1974; Watson and Blanchard, 1984; Xu *et al.*, 1996; Pielke *et al.*, 1999). For example, Blanchard and Lopez (1985) found basic recurring patterns, depending upon thermodynamic properties and changes in the synoptic-scale wind. According to them, convection on any particular day over south Florida is the result of the complex interaction of many scales including the regional (global) scale (Atlantic high pressure circulation), the synoptic scale (waves and fronts), the peninsular scale (sea and lake breezes), and the local scale (heterogeneous soil/vegetation and cloud interactions). Moreover, Lake Okeechobee can have an effect on south Florida's mesoscale weather (*e.g.*, Boybeyi and Raman, 1992), and lake breezes themselves are also sensitive to background atmospheric conditions.

Nicholls *et al.* (1991) showed that soil moisture affects the intensity and evolution of the sea-breeze circulations. They used a two-dimensional model to examine the evolution of sea breeze over Florida, and found that drier soils produce larger sensible heat fluxes than moist soils. These heat fluxes can lead to greater vertical mixing and heating of the atmospheric boundary layer, leading to enhanced convergence of opposing west coast and east coast sea-breezes over the Peninsula. Kingsmill's (1995) observational study showed that convection associated with a sea-breeze and its associated gust front depends upon the vertical depth and horizontal orientation of this front. This work showed the importance of boundary layer processes, which themselves depend upon the soil moisture.

Soil moisture distribution has also been shown to affect other dynamically driven circulations (Pielke *et al.* 1997) and landscape generated circulations (*e.g.*, Pielke *et al.*, 1991; Avissar and Chen, 1993, and Mahrt *et al.*, 1994). Chen and Wang (1995) found that clouds and rain can modify the surface thermal field of Hawaii, resulting in changes in the timing of wind shifts from downslope to upslope flow in the early morning. Clouds and rain also affected the intensity of the upslope flow during the afternoon. In addition, Lyons *et al.* (1995) found that soil moisture significantly affected the intensity

of a Lake Michigan breeze. Shaw *et al.* (1997) showed the use of realistic heterogeneous soil moisture and vegetation may be necessary for the accurate prediction of dryline formation and morphology.

Here, the Penn State/National Center for Atmospheric Research (PSU/NCAR) MM5 mesoscale model (Dudhia, 1993; Grell *et al.*, 1994) is configured to use the Parameterization for Land-Atmosphere Convective Exchange (PLACE) and an improved turbulent kinetic energy (TKE) predicting turbulence parameterization. The former was developed at NASA (Wetzel and Boone, 1995), while the latter was developed at Penn State University (Shafran *et al.*, 1999; Stauffer *et al.*, 1999). To demonstrate the utility of the new model, hereafter referred to as MM5 TKE-PLACE, we simulated the evolution of Florida sea-breeze moist convection on 27 July 1991, during the Convection and Precipitation Electrification Experiment (CaPE).

In Section 2, we describe the model and methodologies for initializing the land surface soil moisture and temperature fields. The experimental design is also presented in Section 2, followed by the CaPE description in Section 3. Model results simulating the evolution of the sea-breeze using explicit cloud physics are shown in Section 4. We used sensitivity tests to investigate the importance of the PBL and land surface parameterizations, along with the soil moisture and temperature initialization. Summary and conclusions are presented in Section 5.

2 Method

a. MM5 Modeling System

The non-hydrostatic PSU/NCAR mesoscale model, widely known as MM5 (Grell et al. 1994, Dudhia 1993) is configured here with two nested grids with horizontal resolutions of 15 and 5 km (the inner nest is shown in Fig. 1). The time-step for the coarse grid was 45 s, while it was 15 s on the fine grid. The two grids are time-dependent and two-way interactive and centered over the Florida Peninsula. There are 23 terrain-following sigma layers in the vertical, the lowest computational layer (surface layer) was about 40 m above ground level, and the highest resolution was in the lower troposphere. Explicit predictive equations are used for grid-resolved cloud water, rain water, and ice (Grell et al. 1994) on both grids, and a subgrid-scale moist convection parameterization (Kain

and Fritsch 1990) is also used on the 15-km coarse grid mesh. Atmospheric and cloud radiative effects are also included.

The model predicts the three-dimensional wind components, temperature, mixing ratios for water vapor, cloud water/ice and rain/snow, and perturbation pressure (p'). The perturbation pressure is the departure from a temporally invariant reference-state pressure described by Dudhia (1993). The default boundary-layer scheme is that of Blackadar (Zhang and Anthes, 1982; Grell *et al.*, 1994), which uses a local first-order closure during neutral and stable conditions, and a non-local first-order closure during unstable (free-convective) conditions.

The alternate scheme used here to represent turbulence processes is a 1.5-order TKE-predicting scheme (Shafran *et al.* 1999, Stauffer et al. 1999) which uses a prognostic equation to compute the local TKE profiles from which the model derives the eddy mixing coefficients used in the vertical diffusion of all the mixing variables. Vertical mixing is performed with liquid water potential temperature and total water mixing ratio due to their conservative properties during phase changes. If ice processes are active, ice-water liquid potential temperature is used and an additional mixing variable for the cloud ice is added to the turbulence parameterization (Stauffer et al. 1999).

The TKE scheme has recently been re-formulated to represent accurately the turbulence in saturated layers (Stauffer et al. 1999). For example, the buoyancy production term in the TKE equation properly accounts for the presence of saturated versus unsaturated layers. This can be important for modeling the interaction of turbulence with explicit (grid-resolved) convection. This work used a version of TKE that did not account for these processes. Future work will examine the effect of this reformulation on simulation results. The turbulence scheme used in this work is hereafter referred to as TKE, and can be used with either the default (SLAB) or alternative (PLACE) land surface scheme.

The default land-surface scheme uses a force-restore method to compute the ground temperature as a function of the soil and vegetation characteristics defined by a look-up table. The surface physical characteristics include albedo, roughness length, emissivity, thermal inertia and soil moisture availability. A surface energy budget equation predicts the ground temperature and includes the effects of turbulent surface fluxes, shortwave and longwave radiation, cloud cover, etc. Thus the ground temperature over land responds

to surface radiative fluxes which vary in time, but the surface characteristics, including the soil moisture, are held fixed in time.

The alternate land-surface scheme, PLACE (Wetzel and Boone 1995), allows soil moisture to change in time, and it interacts with evaporative processes, rainfall, runoff and drainage during the simulations. PLACE calculates surface fluxes of momentum, heat and moisture from soil and vegetation, as well as evaporation of dew and evaporation and throughput of rainfall. It also computes the fluxes of heat and moisture within the ground and drainage of water to bedrock. The soil component of PLACE has five model layers for soil moisture (the top four layers extend up to 1 m in total depth) and seven for temperature (the top five layers extend up to 1 m in total depth). The vegetation component is represented as a single layer that accounts for vegetation type, leaf area index, fractional vegetation cover, etc. Vegetation responses, such as stomatal resistance, evolve from their initial state because of changes in soil moisture, solar flux and atmospheric moisture deficit. The PLACE calculations are performed once every 3 minutes in the model for computational efficiency. The PLACE-derived surface fluxes used by the boundary-layer module are held fixed during this 3-minute period.

b. Experimental Design

The MM5 is initialized at 00 UTC 27 July 1991, and integrated for 24 h until 00 UTC 28 July 1991. Initial and lateral boundary conditions are specified on the 15-km coarse grid mesh via an objective analysis performed at 12-h intervals, using conventional data and National Center for Environmental Prediction (NCEP) spectral analyses. The land surface is usually initialized using the standard MM5 preprocessor in which the surface characteristics are specified as a function of land type via a look-up table. The PLACE vegetation model, though, requires additional parameters that the preprocessor does not provide. For this reason, data from the International Satellite Land Surface Climatology Project (ISLSCP, Meeson *et al.*, 1995) were used to obtain values of fractional vegetation cover and leaf area index, albedo and surface roughness. To do so, we equate vegetation types and soil types with land types given by the MM5 preprocessor. Variables such as thermal conductivity and emissivity of the ISLSCP-provided types were derived from values commonly available in the literature.

Model results are known to be sensitive to initial soil moisture and temperature condi-

tions. Most simulations with MM5 are made using the MM5 preprocessor, which provides climatological values of soil moisture availability*, while the soil temperature is based on temporally averaged surface air temperatures. We created an alternate soil moisture and temperature initialization by running PLACE off-line forced by observations prior to the case date. The off-line PLACE was forced with wind, precipitation, temperature and moisture surface-layer fields from the National Climatic Data Center (NCDC) and CaPE Portable Automated Mesonet (PAM) observations.

Figure 1 shows the initial soil moisture and temperature fields obtained at the 30 observation data points, after interpolation to the model nested grid using a linear interpolation technique. This was also done on the coarse grid, but these results are not shown. For comparison, Fig. 1 also shows the soil moisture and temperature fields obtained from the default MM5 preprocessor (after converting from the MM5 soil moisture availability to soil moisture). Since the default land surface scheme uses the top soil layer temperature and moisture, these fields are shown for them in Fig. 1. However, the soil moisture in one of the root zone layers is shown for PLACE, since this affects the latent heat flux from vegetation (which is usually larger than that from the soil surface). Note that the PLACE derived fields contain two regions of relatively dry soil with warm soil temperatures. There are also two maxima in soil moisture, corresponding to relatively cool initial soil temperatures. These fields are quite different from those based on climatology and those defined by the default MM5 preprocessor. Thus, the PLACE-derived soil moisture and temperature initialization shows much greater heterogeneity than that from the default MM5 initialization.

Table 1 presents a total of eight simulations used to investigate the utility of PLACE and TKE in MM5 for simulation of the Florida sea breeze and Lake Okeechobee circulation. Each experiment represents a different combination of 1) initial conditions for soil temperature and moisture†, 2) land-surface scheme and 3) atmospheric turbulence scheme. The Blackadar PBL is denoted by "HIR" and the TKE turbulence scheme is denoted by "TKE". Following the hyphen in the experiment name, "SLAB" indicates

*Of course, this default scheme does not automatically account for antecedent precipitation in the specification of initial soil moisture in the model

†The moisture availability for runs with PLACE derived off-line soil moisture was obtained by dividing the difference between the PLACE derived soil moisture and the wilting point by the difference between field capacity and wilting point.

the use of the force-restore land surface scheme and "PLACE" denotes the use of the PLACE land-surface model. Finally, the use of a "0" in the experiment name indicates the use of the default soil moisture based on climatology and soil temperature based on a temporal mean of the surface air temperature. No "0" in the name indicates use of the off-line PLACE-derived soil moisture and temperature fields.

The goal of this study is to investigate whether there is added value by coupling the PLACE and TKE schemes to MM5. We will use both subjective (qualitative) and objective (statistical) analysis, a methodology that is commonly applied to evaluating mesoscale model simulations (e.g., Pielke, 1984; Shaw et al. 1997).

3 Case Description

The day of 27 July 1991 from CaPE was a type III day (Blanchard and Lopez 1985), which has a prevailing westerly wind. Typical of such a day, convective clouds formed first at 16 UTC 27 July 1991, along the west coast sea breeze and then later by 18 UTC, along the east coast sea breeze front (Fig. 2). At 18 UTC the edge of convective clouds along the west coast sea breeze had reached the center of the Peninsula, and typical of days with westerly flow, the east coast sea breeze front had made relatively little progress westward (against the prevailing wind).

Fankhauser et al. (1995) and Halverson et al. (1996) produced two-dimensional simulations of CaPE convective events. Their studies explain the physical processes leading to convection during the CaPE experiment, including 27 July 1991. These studies and Wilson and Megenhardt (1997) (observational study) documented the convergence of west coast sea-breeze convection lines with east coast sea-breezes, leading to major thunderstorm development. Here, at 20 UTC 27 July 1991, a squall line of thunderstorms developed just in front of the west coast sea-breeze front. From 20 to 22 UTC, the convergence of this squall line with the east coast sea-breeze front led to relatively strong convection over the eastern half of the Florida peninsula. A region of stratiform clouds formed along the eastern half of the peninsula from 22 to 23 UTC.

Lake Okeechobee also had a strong influence on convection over the peninsula. First, there was developing, but relatively weak convection southeast of Lake Okeechobee. Then, during the dissipation of this convection, convective clouds formed first to the

lake's southwest (19 UTC), and then to the northeast of the lake shore (20 UTC). The convection to the southwest of the lake then expanded northward to off the lake's western and northwestern shore. Between 20 UTC and 21 UTC, the intensity of the convection west of the lake increased because of a merger between it and a sea-breeze front moving inland from the southwest coast. Also, at 20 UTC the lake-breeze front moving northeast of the lake interacted with a sea-breeze front moving westward from the east coast of the Pensinsula. This led to a sharp increase in the intensity of the convection along the northeast shore by 21 UTC. This convection then merged with the convection located to the northwest of the lake shore (between 21 to 22 UTC), leading to a rather large convective cloud stretching from west-to-east, north of the lake.

Figure 3 shows pressure, temperature, and wind obtained from PAM sites and National Weather Service sources (14 data points). Surface pressures over the Peninsula dropped quite substantially from 15 UTC to 18 UTC (10 to 13 LST), especially over the north and central part of the Peninsula, in association with warming surface temperatures that increased, in general, from 28 C to 31 C. For example, at locations over central Florida the pressure dropped 1.5 - 2 mb during this time period. Note, in locations where PLACE indicated relatively dry soil (*i.e.*, < 0.18 mm^3 mm^{-3}), the average increase in temperature was 2 K, but in locations where PLACE indicated relatively moist soil, the average increase in temperature was 1.1 K.

At 15 UTC, the horizontal wind observations do not clearly indicate the sea-breeze fronts apparent in the satellite pictures at 16 UTC. This is probably because of convection occuring right over the observing stations, *e.g.*, Tampa on the west coast. The satellite picture suggests that at 15 UTC the west coast sea-breeze front is located just inland from the west coast, but by 18 UTC it has progressed further eastward towards the center of the peninsula. However, note the development of easterly winds along the east coast from 18 UTC to 21 UTC. These observed winds do show the east coast front, and its westward propagation during this time period.

Observations at 15 UTC also showed relatively large dew points across much of the Peninsula, ranging from 23 to 25 C. But, by 18 UTC, dew points range from 22 to 23 C, from one observational site to another over the drier center of the Peninsula. Dew points have dropped because of relatively small latent heat flux from dry soils and mixing of surface moisture vertically into the PBL. Along most of the east central coast and over

the north (where the soil is wetter), the dew points range from 22 to 25 C. Here, there was a larger latent heat flux than from the dry ground, and vertical mixing was less than over the dry ground because of smaller sensible heat flux. Note, however, that the data points near the coast could have had higher dew points because of the influence of marine air.

At 21 UTC, Fig. 3 shows that the winds have become relatively calm over the central Peninsula, with convective outflow winds pointing to the south and west over two locations. Surface temperatures have cooled substantially over the central Peninsula, indicating the passage of the west coast front. At 24 UTC, the convection has terminated over all but the eastern shore, and surface observations show a decrease in temperature and rise in pressure and dew point at many observation sites. Note, the prevalance of westerly winds, indicating that the west coast sea-breeze front has moved across the Peninsula.

Figure 4 shows accumulated rainfall, tabulated from National Climatic Data Center and PAM sites, for the periods 18 – 21 UTC on 27 July and from 21 to 00 UTC on 28 July. Each field was obtained after interpolating with a Barnes interpolation scheme (Barnes, 1964). From 18 - 21 UTC, areas of western Florida received the most rainfall. In contrast, from 21 UTC on 27 July to 00 UTC on 28 July, the largest amount of accumulated rain occurred over south central and eastern Florida. The rainfall maxima during each time period correspond well with the sequence of satellite pictures, although the rain gauge network cannot capture the convection shown to the southwest and northeast of Lake Okeechobee. Notice the relatively large magnitude (50 mm) of measured rainfall over east-central Florida in a three hour timespan.

4 Results

a. MM5 TKE-PLACE and MM5 HIR-SLAB 0

In this section, we compare results from a simulation, TKE-PLACE, that contains the new model sub-components and PLACE off-line derived initial conditions with HIR-SLAB 0, which contains none of these.

Pielke (1984) discusses the methods available for comparing different model simulations. One is to show qualitative agreement between model simulated fields and obser-

vations, while a second is to apply statistical tests to quantify the model results (see, for example, Pielke (1984) and Shaw *et al.* (1997)). This study used four sets of observational data to evaluate the model results: i) the surface fluxes at observational sites (2 points), ii) the surface observations (37 points), iii) area-averaged rainfall (63 points), and iv) fractional cloud cover (almost complete coverage of simulated domain).

Figure 5 shows the sensible heat fluxes obtained with MM5 HIR-SLAB 0 and MM5 TKE-PLACE at 15 UTC, for the nested domain (hereafter, the names for the different model versions do not contain the "MM5" acronym). Note, SLAB was initialized using soil temperature and moisture data provided with the MM5 preprocessor. PLACE was initialized using soil moisture and temperature fields derived from off-line simulations of the PLACE model itself.

The model simulations have different distributions of sensible heat fluxes at 15 UTC, corresponding mostly to the distribution of soil moisture in each. HIR-SLAB 0 had a relatively uniform distribution of sensible and latent heat flux. In contrast, areas that had relatively dry ground in TKE-PLACE produced strong sensible heating, while areas that had relatively moist ground produced strong latent heating. As noted by Shaw *et al.* (1997), the partitioning of the net radiation balance at the surface responds most strongly to the soil moisture distribution because the equilibrium time-scale for soil moisture is longer than for soil temperature. Because the surface fluxes were very small by the beginning of the solar day (about 12 hours after each simulation began), the TKE-PLACE initial surface temperature, which is shown in Fig. 1, had likely little impact on the development of daytime surface fluxes.

The modelled data were compared to observations of surface flux data (two data points located on Cape Canaveral along the northcentral coast). We have averaged this data and model data over an area about the size of the Cape, and show the results in Fig. 6. An analysis of the simulated fluxes at each site showed the importance of the initial boundary conditions and vegetation in partitioning the net radiation between upward (sensible and latent) heat flux and downward ground flux. It suggests that the initial soil moisture was too large in each model simulation (Note, PLACE, however, had a very strong gradient of soil moisture from the Cape to inland over the peninsula). Yet, TKE-PLACE model produced more realistic sensible heat fluxes than HIR-SLAB 0, while producing similar latent heat fluxes to HIR-SLAB 0. Note, the TKE-PLACE model

would have produced more sensible heat flux if cloud cover had not erroneously limited the net radiation during the middle of the afternoon. Without the PLACE derived soil temperature and overlying vegetation, the SLAB model produced too much ground flux (not shown) and too little sensible heat flux. Certainly, the SLAB model would have produced more realistic heat fluxes with the PLACE initializiation of soil moisture and temperature (but, we show later on that this alone, without, for example, vegetation covering the ground, is not enough to produce a better simulation of the sea-breeze).

Table 2 shows that TKE-PLACE produced smaller (average) local biases than HIR-SLAB 0. The former had a ranking of 3 (out of a possible 8) while the latter had a ranking of 5. TKE-PLACE had a positive wind bias (a rank of 5), which might be one reason TKE-PLACE produced too much surface latent heat flux. On the other hand, HIR-SLAB 0 produced about the same latent heat flux, but it had a very small wind bias (a rank of 1). Thus, it is likely that both station were initialized with too high a moisture availabilty. Note, also, that TKE-PLACE produced a ranking of 1 for wind direction, while HIR-SLAB 0 produced a ranking of 5. This relatively poor ranking of HIR-SLAB 0 occurred because HIR-SLAB 0 produced a relatively weak moist convection (owing to relatively small surface sensible heat fluxes).

Table 3 shows that TKE-PLACE produced smaller (average) domain biases than HIR-SLAB 0. The former had a ranking of 3 (out of a possible 8) while the latter had a ranking of 5. TKE-PLACE produced relatively high rankings in dew point and wind direction, while HIR-SLAB 0 did not. TKE-PLACE ranked fourth in wind speed, but had a larger cold bias (a lower ranking) than HIR-SLAB 0. Based on the dew point biases, TKE-PLACE produced better latent heat fluxes than HIR-SLAB 0. Moreover, the cold bias in TKE-PLACE developed after the onset of moist convection (suggesting that the model simulate too much evaporative cooling in the lowest model layers). This leaves open the possibility that TKE-PLACE produced better agreement between the observed and modelled sensible heat fluxes. Possible support for this position can be found by noting that TKE-PLACE produced a very high ranking for wind direction.

We did not have a data set that could be used to verify the soil moisture and initial temperature fields that produced the heat fluxes discussed above. However, we have some confidence in these initial fields because the biases of the surface variables were better represented by TKE-PLACE than HIR-SLAB 0.

A comparison with observations showed that TKE-SLAB produced more rain and more realistic rainfall than HIR-SLAB 0. TKE-PLACE produced about 4 times as much rain as TKE-SLAB 0; TKE-PLACE's number average was 10.25 and its area average was 8.96. Table 4 shows that TKE-PLACE had a relatively high ranking, while HIR-SLAB 0 had the lowest ranking.

TKE-PLACE did much better than HIR-SLAB 0 in simulating the observed cloud fraction. Figures 7 and 8 show simulated cloud condensate from the HIR-SLAB 0 and TKE-PLACE simulations, respectively. Comparing these figures with Fig. 2, TKE-PLACE produced a much better simulation of cloud cover, including i) convective cloud development at 16 UTC and 17 UTC; ii) a line of convective cells moving eastward with the west coast sea-breeze at 18 UTC; iii) a line of convective cells moving westward with the east-coast sea-breeze (somewhat west, though, of their actual position); and iv) the timing and location of convection over Lake Okeechobee. These features were not reproduced by HIR-SLAB 0.

Figure 9 shows a scatterplot of observed versus modelled fraction cloud cover. The observed fractional cloud amount was obtained by simply adding up the satellite pixels with cloud and dividing by the total number of pixels on the peninsula. The modelled fractional cloud cover was determined by counting the number of model grid-elements with cloud amount above a threshold value and dividing by the total number of grid-elements on the peninsula within the nested domain (this calculation was done three times with different threshold values and averaged to minimize the effect on the analysis of arbitrarily choosing a threshold value). It shows that TKE-PLACE produced many more points within 25% of the observations than HIR-SLAB 0. Note, also, that HIR-SLAB 0 had a relatively large negative bias (see also Fig. 7).

Table 2 summarizes the statistics for the scatter plot of Fig. 9, by showing the domain-averaged cloudiness and root mean square error. Two measures of root mean square error are shown in Table. 2. The first indicates the model skill in obtaining the timing of the domain averaged fractional cloudiness (RMS_1), while the latter indicates the model skill in obtaining the correct timing and location of cloud cover within 8 sub-domains of the Peninsula (RMS_2). TKE-PLACE produced much better total cloud cover and much smaller values of RMS_1 and RMS_2 than HIR-SLAB 0.

b. Sensitivity Tests

Briefly, we compare and contrast the results from all 8 simulations. Our goal is to quantify the effect of model changes discussed above. Factor separation analysis is used to explain model sensitivities.

Importance of PLACE

At the station on the Cape, Table 2 shows that the four simulations with PLACE had the highest average ranking; thus the simulations with PLACE had the lowest biases at the Cape station. Table 3 shows that the PLACE had the highest ranking of all 8 simulations. Thus, these simulations had the smallest (average) bias in the simulation of the surface variables.

The important effect of the PLACE model on the surface fluxes can be seen by examining the biases and rankings for dew point and wind speed. Table 3 shows that the simulations with PLACE produced smaller pressure, temperature and dew points biases than those without PLACE and wind speeds closer to observations.

In regard to rainfall, the simulations with the PLACE model outranked (in the total of the average) the simulations without the PLACE initialization 13 to 18, but did worse than simuations with TKE. In addition, Table 5 shows that the simulations with the PLACE model produced more cloud condensate and smaller root mean square errors than simulations without (*i.e.*, the 0 simulations), but less than with TKE. These results could have important implications for modelling surface hydrology and radiation supporting the use of PLACE-like models in mesoscale atmospheric models.

Importance of TKE

The TKE sub-component model was required to produce the most realistic mesoscale dynamics and moist convection. The simulations with TKE produced better mean wind direction than the other simulations (*e.g.*, PLACE and the 0 simulations). Here, the sum of the average rankings was 13 compared to 18 for the other simulations. These simulations also produced higher rainfall than those without TKE. The sum of the average rankings with the former was 10, as compared to 13 for PLACE and 18 for simulations 0. Also, Table 5 shows that the simulations with TKE produced more cloud cover and

smaller root mean square error than the similations without TKE.

At the local Cape station, the simulations with TKE distinguished themselves only in regard to wind direction (Table 2). This is a function of the dynamics of the convection, forcing the development of the sea-breeze fronts. Table 3 shows that similar results were obtained when comparing biases and rankings at all PAM sites. Moreover, TKE had a colder bias than simulations without TKE (as the absolute value shown equals the negative of the modelled value). Thus, the implementation of the TKE scheme without accounting realistically for the effect of surface initial conditions and vegetation on the surface heat fluxes does not lead to an improvement in the simulation of the surface variables. Here, however, the cold bias was probably due to the need to improve the representation of evaporative cooling from rainfall in the MM5 model, rather than to change the TKE formulation.

Importance of initial soil boundary conditions

Table 2 shows that simulations without the PLACE off-line derived boundary conditions did worse than simulations with PLACE (which include two simulations with the PLACE boundary conditions). Table 3 shows very similar results. In fact, Table 3 also shows that the simulations with PLACE are required to simulate more realistic surface pressure, as well as surface temperature and surface dew point. This lends further support to the PLACE providing a better initialization of soil moisture and soil temperature.

These simulations also suggest the importance of surface heat fluxes on cloud cover and rain. The similations without the PLACE off-line boundary conditions produced a lower ranking for rainfall than those without, *e.g.*, 18 versus 10 for TKE. These simulations also produced the least amount of cloud cover and highest root mean square error than the other simulations.

Factor separation analysis

To better elucidate the importance of PLACE and TKE we used the factor separation technique of Stein and Alpert (1993). The factor separation technique can be used to quantify individual and joint (or synergistic) contributions from model processes (*i.e.*, factors) that affect simulations (*e.g.*, Alpert and Tsidulko (1994)). Here, the relevant factors are i) the PLACE off-line derived soil moisture and temperature fields, ii) the

PLACE land surface model, and iii) TKE boundary layer scheme. Factor separation for three factors require 8 (=2^3) simulations (Table 1), which produces all 8 possible contributions. Note, model simulation depends on a number of factors, *e.g.*, solar radiation, advection, topography, etc, which we do not choose to formally express as individual contributions. When MM5 is used with these "unnamed" factors without the three factors cited above, their combined contribution is expressed as the "zero" contribution. This is, hereafter, referred to as the control case, and, of course, is entitled as simulation HIR-SLAB 0.

The eight contributions are calculated as follows (X is any contribution and Y is a simulation):

$$X(0) = Y_{\text{HIR-SLAB 0}} \tag{1}$$

$$X(1) = Y_{\text{HIR-SLAB}} - Y_{\text{HIR-SLAB 0}} \tag{2}$$

$$X(2) = Y_{\text{HIR-PLACE 0}} - Y_{\text{HIR-SLAB 0}} \tag{3}$$

$$X(3) = Y_{\text{TKE-SLAB 0}} - Y_{\text{HIR-SLAB 0}} \tag{4}$$

$$X(1,2) = Y_{\text{HIR-PLACE}} + Y_{\text{HIR-SLAB 0}} - (Y_{\text{HIR-SLAB}} + Y_{\text{HIR-PLACE 0}}) \tag{5}$$

$$X(1,3) = Y_{\text{TKE-SLAB}} + Y_{\text{HIR-SLAB 0}} - (Y_{\text{HIR-SLAB}} + Y_{\text{TKE-SLAB 0}}) \tag{6}$$

$$X(2,3) = Y_{\text{TKE-PLACE 0}} + Y_{\text{HIR-SLAB 0}} - (Y_{\text{HIR-PLACE 0}} + Y_{\text{TKE-SLAB 0}}) \tag{7}$$

$$\begin{aligned} X(1,2,3) \;=\; & Y_{\text{TKE-PLACE}} - Y_{\text{HIR-SLAB 0}} \\ & - (Y_{\text{TKE-SLAB}} + Y_{\text{HIR-PLACE}} + Y_{\text{TKE-PLACE 0}}) \\ & + (Y_{\text{HIR-SLAB}} + Y_{\text{HIR-PLACE 0}} + Y_{\text{TKE-SLAB 0}}) \end{aligned} \tag{8}$$

Note, we can calculate contributions from the three factors for any model output Y variable.

Sea-breeze development depends upon the air temperature contrast between land and ocean. Furthermore, it can be affected by perturbations in temperature over the peninsula itself, between for example, the southern half and northern half. Here, we examine how the first two factors (PLACE initialization and PLACE land surface model) contributed to the spatial variability of the perturbation potential temperature, θ'. The variable θ' was calculated by subtracting the modelled potential temperature from the

horizontally averaged potential temperature. We chose the time of 17 UTC, since this was after the development of the convective PBL, but prior to the development of clouds in the model simulations. Note, the original fields of temperature were obtained from the temperature of the closest model layer to the ground surface (40 m). The contributions to the perturbation fields are referred to as $X_{\theta'}$ (), where the information within the brackets indicates which factors went into calculating θ'.

Two factors produce 4 contributions to θ', which are shown in Figure 10. In the control case, $X_{\theta'}$ (0) has, with one exception, maxima of 1 to 2 K over a broad part of the Florida peninsula. Here, the uniform initial soil moisture field produced a uniform field of perturbations. In contrast, the contribution from the first factor, as represented by $X_{\theta'}$ (1), correlated closely with the spatial distribution of dry soil. Here, the maxima in $X_{\theta'}$ (1) were as large as 4 K, and represent an additional perturbation in temperature on top of that contribution represented by $X_{\theta'}$ (0). In constrast, $X_{\theta'}$ (2), showed that the type of (PLACE) vegetation can also have an important affect on temperature. It had relatively large values over the northern half of the peninsula, where there is a predominance of broad-leaf and coniferous forest. The most important effect of the joint interaction of both factors occurred over west central Florida. This region showed relatively large values of $X_{\theta'}$ (1,2) ranging up to 3 K. The combination of relatively small soil moisture and vegetation led to warming of the surface layer in locations other than obtained with either factor alone.

Based on the discussion directly above, one can surmise the importance of PLACE and the off-line surface moisture and temperature boundary conditions. Each factor contributed importantly to the perturbation temperature. Thus, we can surmise that these factors would affect the complete set of surface variables. As noted above, simulations with both PLACE or the PLACE derived off-line boundary conditions produced the most realistic biases in the surface variables such as pressure, wind speed and dew point. Clearly, both factors 1 and 2 had an important effect on the surface variables.

The development of cloud condensate depends upon the vertical transport of heat and moisture; one measure of this is the relative humidity (RH), which, at 1.5 km, shows clearly the importance of each individual factor. Figure 11 shows that contributions from the control, the soil moisture distribution, and PLACE (*i.e.*, X_{RH} (0),X_{RH} (1) and X_{RH} (2)) have a spatial pattern very similar to the surface heating in each. The

HIR parameterization transports heat and moisture upwards into the PBL in proportion to the heating of the surface layer, using a non-local, first order parameterization for unstable (free-convective) conditions. Quite interestingly, X_{RH} (3) had maxima along the southwest coast and across the center of the Peninsula. Across the center, the TKE had larger turbulent transport of moisture than than HIR-SLAB 0, which was located in an area that had about half the heat flux of other locations within the domain. Thus, other factors than bouyancy triggered transport might have been important, *i.e.*, such as mechanically driven turbulence (Atkins *et al.*, 1995). One can surmise the relevance of each factor to the possible development of cloud condensate from this figure. Thus, simulations using either PLACE, the off-line derived surface boundary conditions, or TKE, showed improvement in cloud cover and rainfall.

To further explore the importance of the factors, this paper examines how they affect contributions to cloud condensate. Each contribution is referred to as $X_{\psi'}$, Figure 12 shows that modifying the model physics with either $X_{\psi'}$ (1) or $X_{\psi'}$ (2) produced relatively little effect on the modelled cloud condensate at 19 UTC. However, $X_{\psi'}$ (1,2) shows that the factors (1) and (2) can (weakly) act jointly to enhance cloud condensate near Lake Okeechobee and along the southeast coast.

The factor $X_{\psi'}$ (3) shows that TKE (alone) contibutes a small increase in cloud condensate; moreover. the importance of TKE (as noted above) can be more readily seen when TKE acts jointly with other factors. For example, comparing $X_{\psi'}$ (1,2) with $X_{\psi'}$ (1,3) shows that the addition of a more realistic boundary layer scheme is more important than the addition of a more realistic land surface scheme. However, it is interesting to also compare the factors $X_{\psi'}$ (1,3) and $X_{\psi'}$ (2,3). This shows that adding the TKE factor with the PLACE off-line soil moisture and temperature produces more cloud cover than adding TKE with the PLACE model alone – thus demonstrating the importance of the PLACE off-line derived initial soil moisture fields on the model solution (as evidenced by the inability of the statistics for the combined TKE simulations to show more realistic surface variables than simulations with HIR). However, $X_{\psi'}$ (1,2,3) shows that all three factors can act synergistically to produce the largest impact on cloud condensate. Thus, the TKE-PLACE produced the largest cloud amount and the best wind direction, which evolved in response to the dynamics of the sea-breeze moist convection.

5 Summary and Conclusions

This paper demonstrates the utility of the newly coupled MM5 TKE-PLACE model, which is the original MM5 mesoscale model coupled to an improved 1.5 order closure, turbulent kinetic energy boundary layer model (TKE) and soil/vegetation land-surface model (PLACE). We compared modeled data both qualitatively and quantitatively to observed data. Overall, eight simulations tested the sensitivity of the MM5 model to combinations of the new and default model physics, and initialization of soil moisture and temperature. The TKE-PLACE model produced more realistic results than the default model, HIR-SLAB 0, including a better simulation of the sensible heat flux, lower biases for surface variables, better rainfall, and more realistic cloud cover. Of the 8 simulations with different factors, TKE-PLACE compared very well when each simulation was ranked interms of biases of the surface variables, and biases in rainfall. TKE-PLACE also produced more realistic cloud cover than other simulations.

Sensitivity tests showed that the physical representation of the boundary layer and land surface affects quite strongly the model results. A factor separation analysis first demonstrated the importance of two factors: the initial soil temperature and moisture, as well as the PLACE model. The initial soil temperature and moisture fields determine the general spatial structure of the surface temperature perturbations, while the PLACE (vegetation) model can strongly modify these fields. Additional analysis showed the importance of the third factor, TKE. The MM5 model required the combined synergistic effect of all three factors to produce its most realistic simulation.

Note, we used the PLACE model to derive the initial soil fields. Unfortunately, such fields are not readily available to modelers and hence need to be developed off-line for model simulations. Furthermore, the soil moisture evolves in time during a model simulation. Simple models such as SLAB do not allow soil moisture to change during simulations, but models such as PLACE do. Moreover, in the absence of vegetation, more heat is likely to be absorbed into the deep soil layers than with vegetation. The use of a soil/vegetation model appears to allow for a better partitioning between upward sensible and latent heat fluxes and downward ground sensible heat fluxes.

The addition of the model subcomponents could likely have additional benefits to weather and climate prediction. Sophisticated land surface models such as PLACE and

higher-order closure models such as TKE should have their greatest benefit in the prediction of warm season, weakly forced synoptic events, including the land-breeze, vegetation breeze, and air mass thunderstorms. PLACE can provide more realistic surface boundary conditions, including the time evolution of the soil moisture and temperature (as well as runoff) than simple SLAB models. TKE can provide better transfer of momentum, heat, and moisture, through the PBL, and within clouds than first-order closure schemes.

Nichols *et al.* (1991) suggested that their work would provide a basis for future, more complex three-dimensional simulations that will include the effects on an irregular coastline, Lake Okeechobee, and directional wind shear. They noted, in particular, that there was some sensitivity of their results to even small variations of the initial conditions, and, thus, to initial soil moisture. Blanchard and Lopez (1985) noted that "it is probably beyond our current understanding to understand completely the myriad factors and complex interactions that determine the exact convective pattern for any particular day." Our results demonstrated the complexity of the three-dimensional response. Yet, with the new version of MM5, which includes the TKE model and PLACE, we identified and better reproduced the "myriad factors and complex interactions" that determined the convection on 27 July, 1991.

Finally, the simluations produced here used a relatively fine resolution for mesoscale modelling. Additional studies are underway to test the modified code at resolutions used often in regional-scale modelling, *e.g.*, 25 to 100 km.

Acknowledgement

The first author was supported by a National Aeronautics and Space Administration Cooperative Agreement NCC 5-82. He thanks Robert Adler and Bill Lau for their support. He would also like to thank Harry Cooper for supplying flux and PAM data from the CaPE experiment site, and Jeff Halverson for providing advice on the CaPE experiment. W.-K. Tao, R. D Baker and Y. Jia are supported by NASA headquarter's (HQ) physical climate program and TRMM. They thank R. Kakar (HQ) for his support. The views expressed herein are those of the authors and do not necessarily reflect the views of Columbia University, The Pennsylvania State University, NASA, or Tel Aviv University.

6 References

Alpert, P. and M. Tsidulko, 1994: "Project WIND - numerical simulations with Tel Aviv Model PSU-NCAR model run at Tel Aviv University." Mesoscale Modeling of the Atmosphere (eds. R.A. Pielke and R.P. Pierce), Meteorological Monographs, **25**, No. 47, Amer. Meteor. Soc., Boston, 81–95.

Atkins, N.T., R.M. Wakimoto, T.M. Weckwerth, 1995: Observations of the sea-breeze front during CaPE. Part II: dual-doppler and aircraft analysis. *Mon. Wea. Rev.*, 944–969.

Avissar, R., and F. Chen, 1993: Development and analysis of prognostic equations for mesoscale kinetic energy and mesoscale (subgrid-scale) fluxes for large scale atmospheric models. *J. Atmos. Sci.*, **50**, 3751–3774.

Barnes, S. L., 1964, A technique for maximizing details in numerical weather map analysis, *J. Applied Meteorol.*, **3,** 396-409.

Blanchard, D. O, and R. E. Lopez, 1985: Spatial Patterns of Convection in South Florida. *Mon. Wea. Rev.*, **113**, 1282 - 1299.

Boone, A., and P. Wetzel, 1996: Issues related to low resolution modeling of soil moisture: experience with the PLACE model. *Global and Plan. Change*, **13**, 161 - 181.

Boybeyi, Z, and S. Raman, 1992: A three-dimensional numuerical sensitivity stufy of convection over the Florida peninsula. *Bound. Lay. Meteorol.*, **60** 325 - 359.

Businger, J. A., J. C. Wyngaard, Y. Izumi, and E. F. Bradley, 1971: Flux-profile relationships in the atmospheric surface layer. *J. Atmos. Sci.*, **28**, 181-189.

Byers, H. R., and H. R. Rodebush, 1948: Causes of thunderstorms of the Florida Peninsula. *J. Meteor.*, **5**, 275 - 280.

Chen, Y.-L., and J.-J. Wang, 1995: The effects of precipitation on the surface temperature and airflow over the Island of Hawaii. *Mon. Wea. Rev.*, **123**, 681 - 694.

Dudhia, J., 1993: A nonhydrostatic version of the Penn-State-NCAR mesoscale model: Validation tests and simulation of an Atlantic cyclone and cold front. *Mon. Wea. Rev.*, **121**, 1493 - 1513.

Fankhauser, J. C., N.A. Crook, J. Tuttle, L. J. Miller, and C. G. Wade, 1995: Initiation of deep convection along boundary layer convergence lines in a semitropical environment, 1995: *Mon. Wea. Rev.*, **123**, 291 - 313.

Grell, G.A., J. Dudhia, and D.R. Stauffer, 1994: A description of the fifth-generation Penn State/NCAR Mesoscale Model (MM5). NCAR Tech. Note, NCAR/TN−398+STR, 122 p.

Halverson, J., M. Garstang, J. Scala, and W.-K. Tao, 1996: Water and energy budgets of a Florida mesoscale convective system: A combined observational and modeling study. *Mon. Wea. Rev.*, **124**, 1161 - 1180.

Kain, J.S. and J.M. Fritsch, 1990: A one dimensional entraining/detraining plume model and its application to convective parameterization. *J. Atmos. Sci.*, **47**, 2784–2802.

Kingsmill, D. E., 1995: Convection initiation associated with a sea-breeze front, a gust front, and their collision. *Mon. Wea. Rev.*, **123**, 2913 - 2933.

Mahrt, L., J.S. Sun, D. Vickers, J.I. MacPherson, J.R. Pederson, and R.L.Desjardins, 1994: Observations of fluxes and inland breezes over a heterogeneous surface. *J. Atmos. Sci.*, 2484 - 2499.

Meeson, B.W., F.E. Corprew, J.M.P. D.M McManus (and many others), 1995: ISLSCP Initiative I-Global Data Sets for Land-Atmospheric Models, 1987 - 1988. Volumes 1 - 5. Published on CD by NASA (USA_NASA_GDAAC_ISLSCP_001-USA_NASA_GDACC_ISLSCP_005).

Lyons, W. A., C. J.Tremback, and R. A. Pielke, 1995: Applications of the Regional Atmospheric Modeling System (RAMS) to provide input to photochemical grid models for the Lake-Michigan Ozone study (LMOS). *J. Appl. Meteorol.*, **34**, 1762 - 1786.

Nichols, M.E., R.A. Pielke, W.R. Cotton, 1991: A two-dimensional numerical investigation of the interaction between sea breezes and deep convection over the Florida peninsula. *Mon. Wea. Rev.*, **119**, 298 - 323.

Pielke, R. A, 1974: A three-dimensional numerical model of the sea breezes over south Florida. *Mon. Wea. Rev.*, **102**, 115 - 119.

Pielke, R. A., 1984: *Mesoscale Numerical Modelling.* Academic Press, New York, 612 pp.

Pielke, R. A., G. A. Dalu, J. S. Snook, T. J. Lee, and T. G. F. Kittel, 1991: Nonlinear influence of mesoscale land use on weather and climate. *J. Climate*, **4**, 1053–1069.

Pielke, R.A., T.J. Lee, J.H. Copeland, J.L. Eastman, C.L. Ziegler, and C.A. Finley. 1997: Use of USGS-provided data to improve weather and climate simulations. . *Ecol. Applic.*, **7**, 3 - 21.

Pielke, R. A., R. L. Walko, L. T. Steyaert, P. L. Vidale, G. E. Liston, W. A. Lyons, and T. N. Chase, 1999: The Influence of Anthroponogenic Landscape Changes on Weather in South Florida. *Mon. Wea. Rev.*, **127**, 1653 - 1673.

Shafran, P.C., N.L. Seaman and G.A. Gayno, 1999: Evaluation of numerical predictions of boundary-layer structure during the Lake Michigan Ozone Study (LMOS). *J. Appl. Meteor.*, (in press).

Shaw, B. L, R. A. Pielke, C. and L Ziegler, 1997: A three-dimensional numerical simulation of a Great Plains Dryline. *Mon. Wea. Rev.*, **125**, 1489 - 1506.

Stauffer, D.R, 1999: In-cloud turbulence and explicit microphysics in the MM5. Workshop on Land-Surface Modeling and Applications to Mesoscale Models. 177 - 180.

Stein, U, and P. Alpert, 1993: Factor separation in numerical simulations. J. Atmos. Sci., **50**, 2107 - 2115.

Watson, A. I., and D. O. Blanchard, 1984: The relationship between total area divergence and convective precipitation in south Florida. *Mon. Wea. Rev.*, **112**, 673 - 685.

Wetzel, P. J, and A. Boone, 1995: A parameterization for Land-Atmosphere- Cloud Exchange (PLACE): Documentation and testing of a detailed process model of the partly cloudy boundary layer over heterogeneous land. *J. Climate*, **8**, 1810 - 1837.

Wilson, J. W., and D. L. Megenhardt, 1997: Thunderstorm initiation, organization, and lifetime associated with Florida boundary layer convergence lines. *Mon. Wea. Rev.* **125**, 1507 - 1525.

Xu, L., S. Raman, R. V. Madala, and R. Hodur, 1996: A non-hydrostatic modeling study of surface moisture effects on mesoscale convection induced by sea breeze circulation. *Meteorol. Atmos. Phys.*, **58**, 103 - 122.

Zhang, D.L., and R.A. Anthes, 1982: A high resolution model of the planetary boundary layer: Sensitivity tests and comparisons with SESAME-79 data. *J. Appl. Meteor.*, 1594 - 1609.

List of Figures

Figure 1: MM5 Model pre-processor provided soil moisture (top left) and soil temperature (bottom left). Off-line simulations of the PLACE model produced soil moisture and soil temperature fields, shown in plots, respectively, at top right and bottom right. The time was 00 UTC 27 July, 1991. Lake Okeechobee is shown at bottom right corner of the Florida Peninsula.

Figure 2: Visible satellite pictures of the Florida peninsula, encompassing the nested domain used in the model simulations. Pictures show a sequence of times on 27 July, 1991: 16 UTC (top left), 17 UTC (top right), 18 UTC (upper middle left), 19 UTC (upper middle right), 20 UTC (lower middle left), 21 (UTC) (lower middle right), 22 UTC (bottom left), and 23 UTC (bottom right). Lake Okeechobee is at the lower right.

Figure 3: Surface data obtained from PAM and National Weather Service reporting stations. Figures show pressure, temperature, dew point, and wind on 27 July, 1991 at 15 UTC (top left), 18 UTC (top right), and 21 UTC (bottom left), as well as 28 July, 1991 at 24 UTC (bottom right). A tail on the station circle indicates a surface wind of 5 m s^{-1}, while a barb on this tail indicates an additional 5 m s^{-1}.

Figure 4: Accumulated rainfall obtained from PAM sites (+) and NCDC observing stations ($\diamond$) on 27 July, 1991 between 18 - 21 UTC (top) and 21 - 00 UTC (bottom). The plots were produced using a Barnes interpolation.

Figure 5: Horizontal distributions of surface sensible (top) and latent heat fluxes (bottom), obtained in MM5 HIR-SLAB 0 and MM5 TKE-PLACE, on 27 July at 15 UTC.

Figure 6: Time dependence of surface sensible heat flux, surface latent heat flux, and surface net radiation obtained in observations (0), HIR-SLAB 0 (1), and TKE-PLACE (8). The units for each are W m^{-2}. There were two observation points located on the Cape along the east central coast, which were averaged to produce

these plots. The model data were averaged over areas corresponding roughly to the size of the Cape.

Figure 7: A plot of vertically integrated cloud condesate over a 1000 m to 8000 m atmospheric layer for HIR-SLAB 0, at the times shown in Fig. 2.

Figure 8: Same as Fig. 2, but for TKE-PLACE.

Figure 9: A scatterplot of observed versus modelled fractional cloud cover for TKE-PLACE (circles) and HIR-SLAB 0 (diamonds). Data points falling along the solid line had no error. The dotted lines indicate the range of 25% error below and above the solid line. See Table 2 for the method used to obtain fractional cloud cover from the observations and model output.

Figure 10: Three contributions to the distribution of surface temperature perturbations ($X_{\theta'}$) and one joint contribution (at 17 UTC). Note, we show only perturbations over land. The top left hand box shows the contributions to θ' from the combined contributions of the original physical subcomponents within the MM5 model; that is without any modifications (referred to in the text as ($X_{\theta'}$ (0)). The contribution from the first factor, or the PLACE (off-line) derived initial soil moisture and temperature fields (shown in Fig. 1), is shown in the top right hand box (referred to as $X_{\theta'}$ (1)). The contribution from the second factor, or the PLACE land surface model, is shown in the bottom left hand box (referred to as $X_{\theta'}$ (2)). The joint contribution from the first and second factors is shown in the bottom right hand corner (referred to as $X_{\theta'}$ (1,2)).

Figure 11: Single contributions to relative humidity (referred to as X_{RH} in the text) at 1.5km and 17 UTC.

Figure 12: Single, joint (J.-C), and synergistic (S.-C.) contributions to cloud condensate (referred to as $X_{\psi'}$ in the text) at 18 UTC.

List of Tables

Table 1: Description of simulations. SLAB is the original, two-layer soil model, and PLACE is a multilayer soil and vegetation land surface model. The number 0 indicates that the model provided soil temperature and moisture fields were used to initial either land surface model. HIR is a first order closure, high resolution (Blackadar) boundary layer model, while TKE is a 1.5 order, turbulent kinetic energy scheme used in calculating boundary layer and cloud subgrid-scale fluxes. Note, we have dropped the acronym MM5 from the list of simulations.

Table 2: The biases and rankings for the station at 28.45 N and 80.52 W (located on Cape Canaveral, on the northeastern shore). The last three rows show the (absolute) sum of the biases and sum of the average rankings from simulations which contain the acronyms listed. Note, the minumum average ranking was three, while the maximum average ranking was 5.

Table 3: Biases and rankings of PAM observational sites. The last three rows show the (absolute) sum of the biases and sum of the rankings from simulations which contain the acronyms listed. Note, the minumum average ranking was three, while the maximum average ranking was 5.

Table 4: Observed, modelled rainfall, and rankings for HIR-SLAB 0 and TKE-PLACE. The first column is the number average, while the second column is the area average (the Peninsula was divided up into the Northwest (NW; 6 observational data points), Northeast (NE; 27 observational data points), Southeast (SE; 24 observational data points), and Southwest (SW; 7 observational data points) quadrants and then the rainfall was area averaged.) The last three rows show the (absolute) sum of the biases and sum of the (average) rankings from simulations which contain the acronyms listed.

Table 5: Average fractional cloud amount obtained in each simulation, percent of modelled versus observed fractional cloud amount, and root mean square (RMS) of modelled versus observed fractional cloud amount. The fractional cloud amount obtained in observations was calculated by first determining the edge of clouds from digitilized satellite data for that shown in Fig. 2. This cloud edge was used to set a minimum reflectance value for cloud pixels. Second, pixels with reflectance values greater or equal to the minimum were summed and then divided by the total number of pixels. The

fractional cloud amount from the model results was obtained by adding up all the pixels with cloud amount greater than a threshold value (when averaged from the surface to 8 km) and dividing by the number of pixels. This was done for three different thresholds, including 0.001, 0.01, and 0.1 g kg $^{-1}$, and then the results were averaged to produce the numbers in Table 5. Two sets of numbers are shown for the root mean square error. In the first (RMS_1), we used cloud amount over the domain of the peninsula (8 total data points, including 16 UTC to 23 UTC). This indicates the model skill in simulating the timing of the "gross" cloud amount. In the second, (RMS_2), we use cloud amount over 8 equally divided quadrants (64 data points, 8 data points per hour). This number indicates the model skill in simulating the timing and location of fractional cloud cover. The last three rows show the averages of each variable from the simulation which contain the acronyms listed. The average fractional cloud amount obtained in the observations was 0.40 for the 8 hours shown in Fig. 2.

Table 1: Description of simulations. SLAB is the original, two-layer soil model, and PLACE is a multilayer soil and vegetation land surface model. The number 0 indicates that the model provided soil temperature and moisture fields were used to initial either land surface model. HIR is a first order closure, high resolution (Blackadar) boundary layer model, while TKE is a 1.5 order, turbulent kinetic energy scheme used in calculating boundary layer and cloud subgrid-scale fluxes. Note, we have dropped the acronym MM5 from the list of simulations.

Acronym	*Description*
HIR-SLAB 0	Original model
HIR-SLAB	Uses soil fields derived from off-line PLACE simulations
HIR-PLACE 0	Uses PLACE instead of SLAB
HIR-PLACE	Uses PLACE, but with soil fields from off-line PLACE simulations
TKE-SLAB 0	Uses TKE instead of HIR
TKE-SLAB	Uses TKE, but soil fields from off-line PLACE simulations
TKE-PLACE 0	Uses TKE and PLACE
TKE-PLACE	Uses TKE and PLACE, but soil fields from off-line PLACE simulations

Table 2: The biases and rankings for the station at 28.45 N and 80.52 W (located on Cape Canaveral, on the northeastern shore). The last three rows show the (absolute) sum of the biases and sum of the average rankings from simulations which contain the acronyms listed. Note, the minumum average ranking was three, while the maximum average ranking was 5.

Acronym	*Pressure (mb)*	*Temp. (K)*	*Dew Point (K)*	*Wind Speed (m s^{-1})*	*Wind Dir.*	*Ranking*
HIR-SLAB 0	0.3	-3.1	-1.2	-0.2	56.3	5
TKE-PLACE	-0.1	-3.1	0.5	0.8	-1.2	3
PLACE	0.60	11.6	0.9	2.4	146.8	13
TKE	0.7	12.7	1.5	3.1	61.0	18
0	0.90	12.6	2.5	1.8	149.9	18

Table 3: Biases and rankings of PAM observational sites. The last three rows show the (absolute) sum of the biases and sum of the rankings from simulations which contain the acronyms listed. Note, the minumum average ranking was three, while the maximum average ranking was 5.

Acronym	*Pressure (mb)*	*Temp. (k)*	*Dew Point (K)*	*Wind Speed ($m\ s^{-1}$)*	*Wind Dir.*	*Ranking*
HIR-SLAB 0	0.6	-1.8	-1.2	0.8	-49.7	5
TKE-PLACE	0.55	-2.8	-0.1	1.0	9.9	3
PLACE	1.5	8.1	1.4	2.9	126.2	13
TKE	2.4	10.2	2.3	6.1	55.0	18
0	2.2	8.6	3.1	3.9	127.8	18

Table 4: Observed, modelled rainfall, and rankings for HIR-SLAB 0 and TKE-PLACE. The first column is the number average, while the second column is the area average (the Peninsula was divided up into the Northwest (NW; 6 observational data points), Northeast (NE; 27 observational data points), Southeast (SE; 24 observational data points), and Southwest (SW; 7 observational data points) quadrants and then the rainfall was area averaged.) The last three rows show the (absolute) sum of the biases and sum of the (average) rankings from simulations which contain the acronyms listed.

Acronym	*number*	*area*	*Ranking*
Observations	9.17	8.96	
HIR SLAB 0	2.06	2.17	8
TKE PLACE	10.25	8.96	1
PLACE	7.9	7.65	13
TKE	11.57	11.99	10
0	6.96	7.37	18

Table 5: Average fractional cloud amount obtained in each simulation (from 16 UTC to 23 UTC), percent of modelled versus observed fractional cloud amount, and root mean square (RMS) of modelled versus observed fractional cloud amount. The fractional cloud amount obtained in observations was calculated by first determining the edge of clouds from digitilized satellite data for that shown in Fig. 2. This cloud edge was used to set a minimum reflectance value for cloud pixels. Second, pixels with reflectance values greater or equal to the minimum were summed and then divided by the total number of pixels. The fractional cloud amount from the model results was obtained by adding up all the pixels with cloud amount greater than a threshold value (when averaged from the surface to 8 km) and dividing by the number of pixels. This was done for three different thresholds, including 0.001, 0.01, and 0.1 g kg $^{-1}$, and then the results were averaged to produce the numbers in Table 5. Two sets of numbers are shown for the root mean square error. In the first (RMS_1), we used cloud amount over the domain of the peninsula (8 total data points, including 16 UTC to 23 UTC). This indicates the model skill in simulating the timing of the "gross" cloud amount. In the second, (RMS_2), we use cloud amount over 8 equally divided quadrants (64 data points, 8 data points per hour). This number indicates the model skill in simulating the timing and location of fractional cloud cover. The last three rows show the averages of each variable from the simulation which contain the acronyms listed. The average fractional cloud amount obtained in the observations was 0.40 for the 8 hours shown in Fig. 2.

Acronym	*fractional cloud cover (model)*	%	RMS_1	RMS_2
HIR SLAB 0	0.12	31	0.40	0.44
TKE PLACE	0.32	80	0.14	0.32
PLACE	0.24	58	0.25	0.35
TKE	0.26	64	0.21	0.34
0	0.19	47	0.31	0.39

MM5 Soil Moisture

PLACE Root Zone Soil Moisture

(mm**3/mm**3)

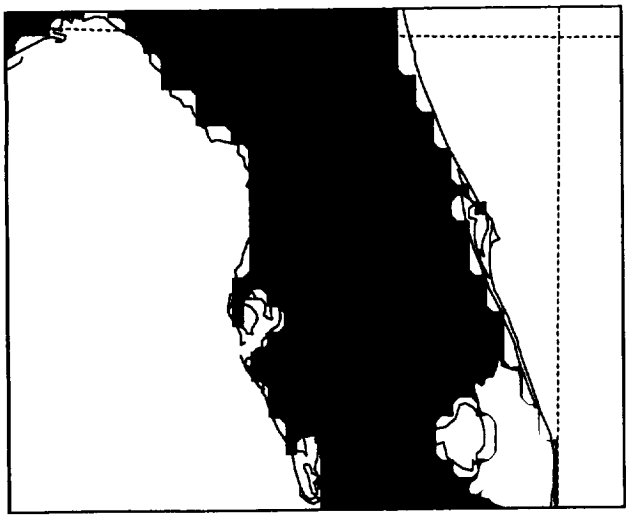

MM5 Soil Surface Temperature

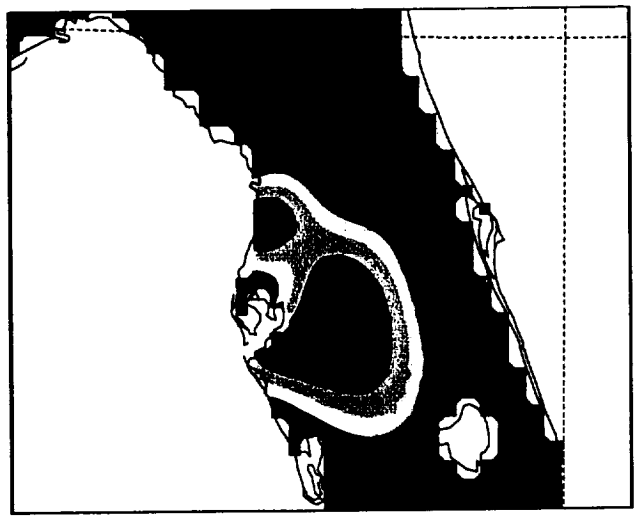

PLACE Soil Surface Temperature

(K)

16 UTC

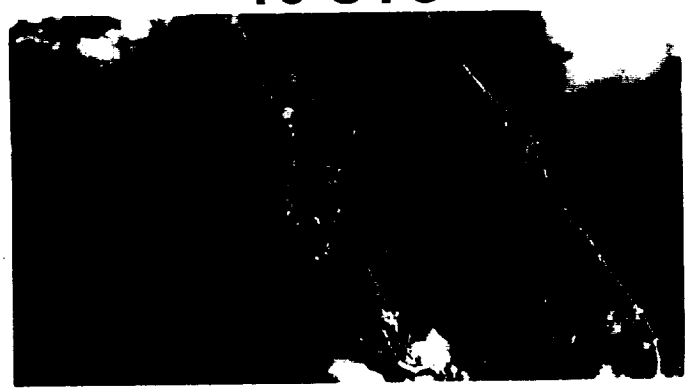

17 UTC

18 UTC

19 UTC

20 UTC

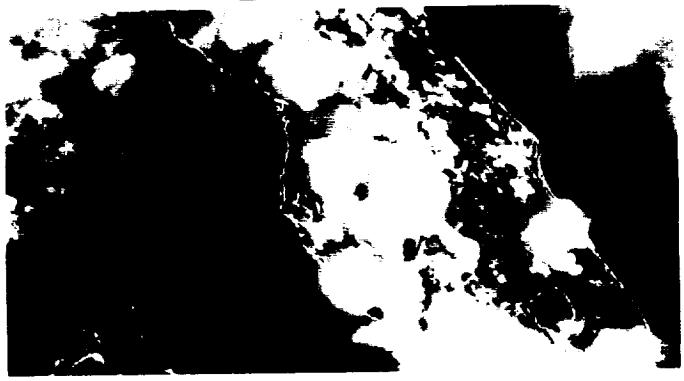

21 UTC

22 UTC

23 UTC

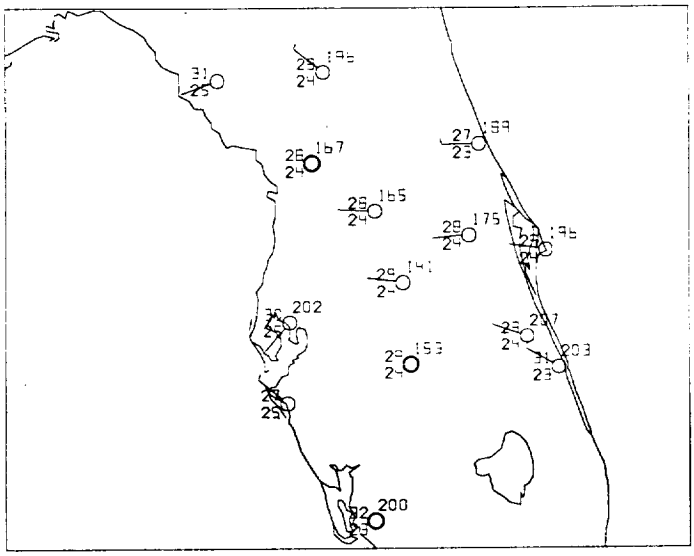

SAT 15Z JL-27-91

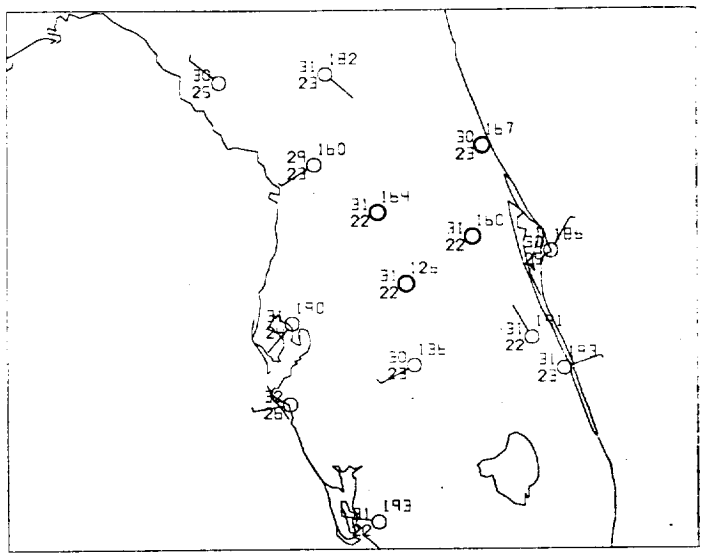

SAT 18Z JL-27-91

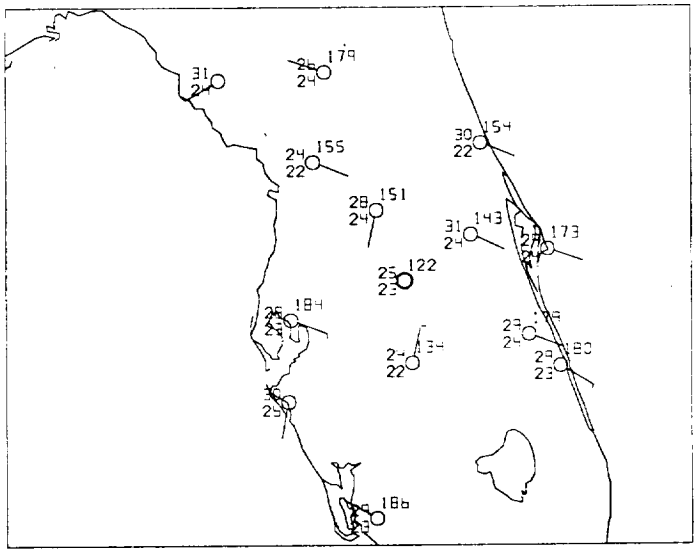

SAT 21Z JL-27-91

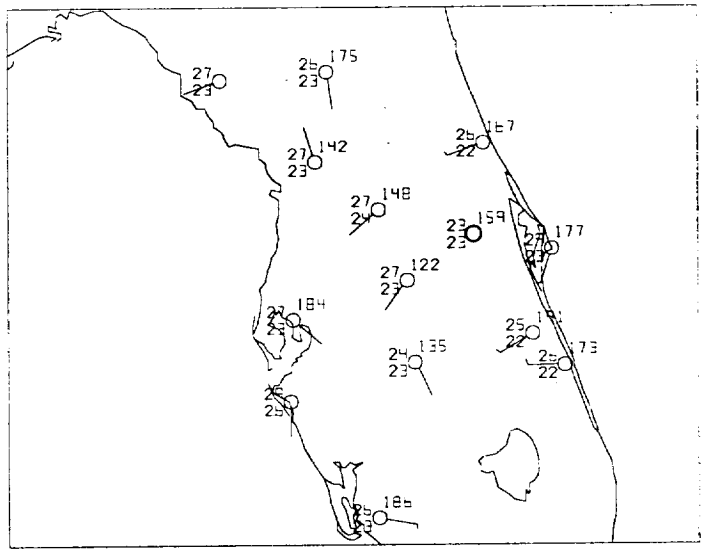

SUN 00Z JL-28-91

a)

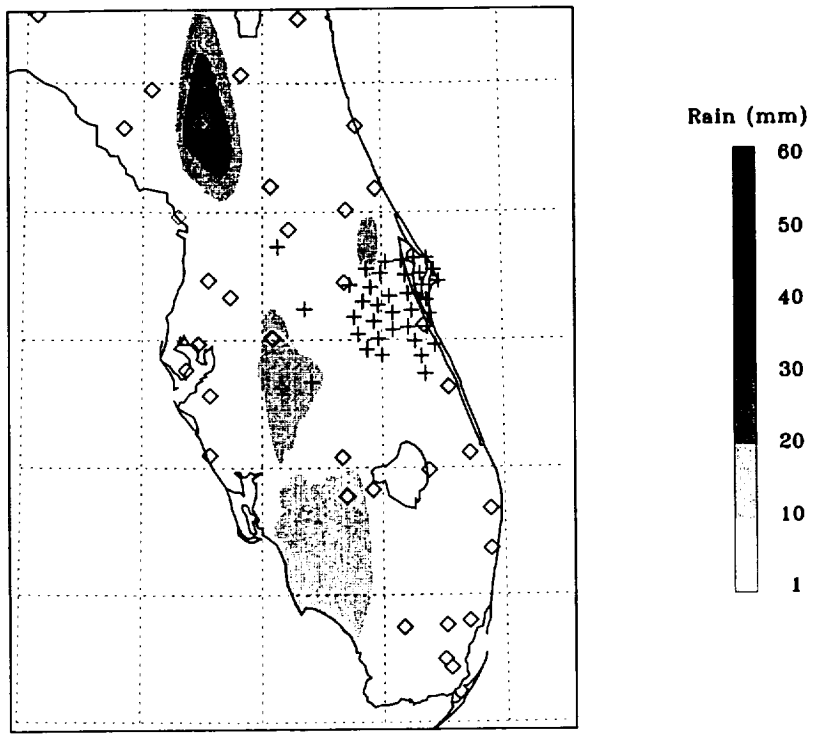

b)

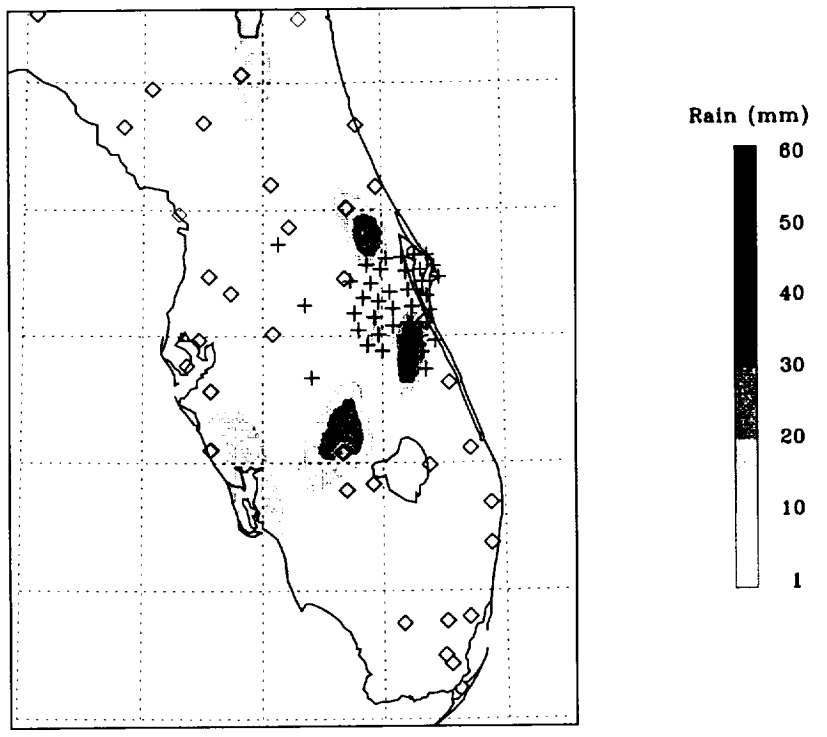

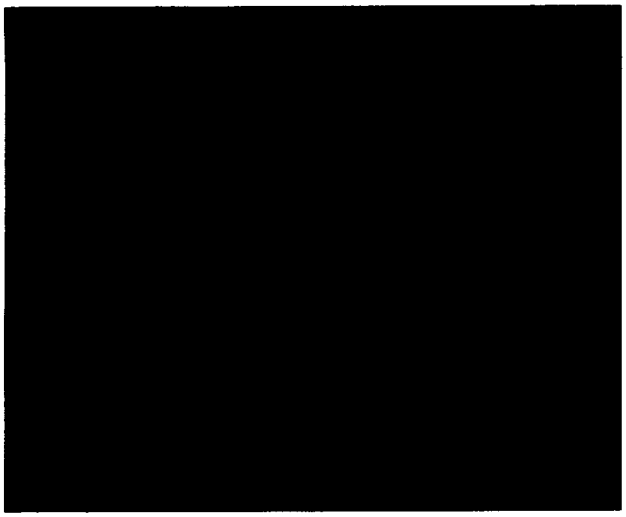

MM5 HIR-SLAB 0 (SENSIBLE)

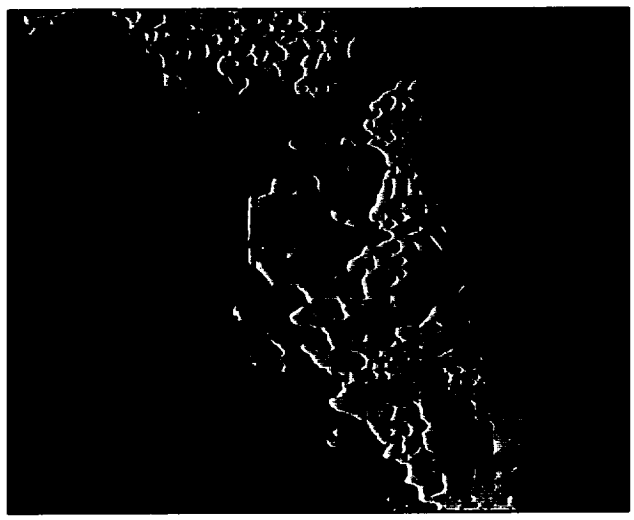

MM5 TKE-PLACE (SENSIBLE)

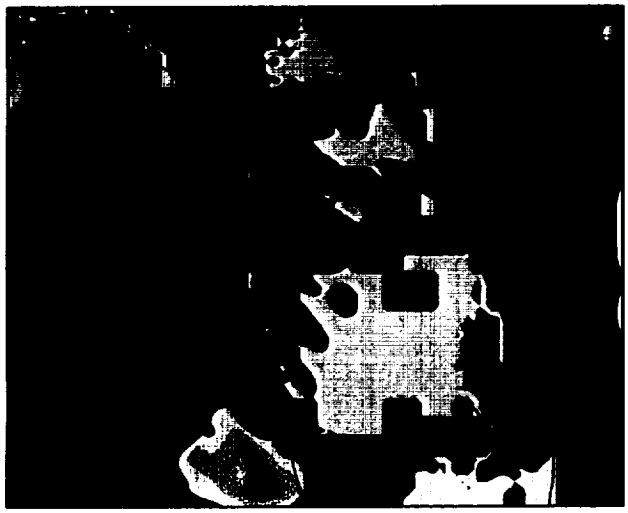

MM5 HIR-SLAB 0 (LATENT)

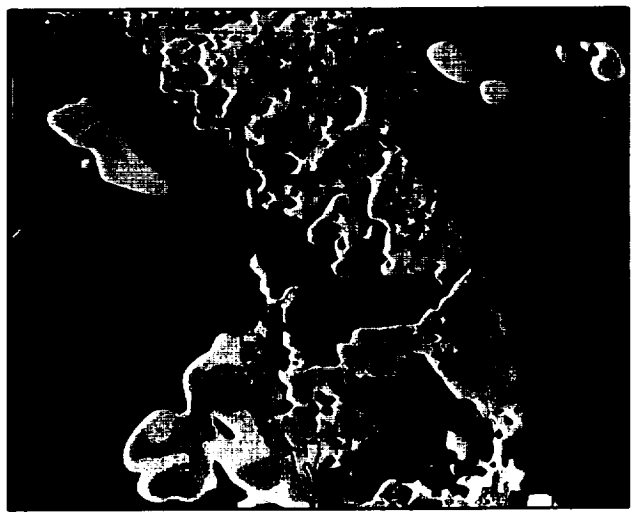

MM5 TKE-PLACE (LATENT)

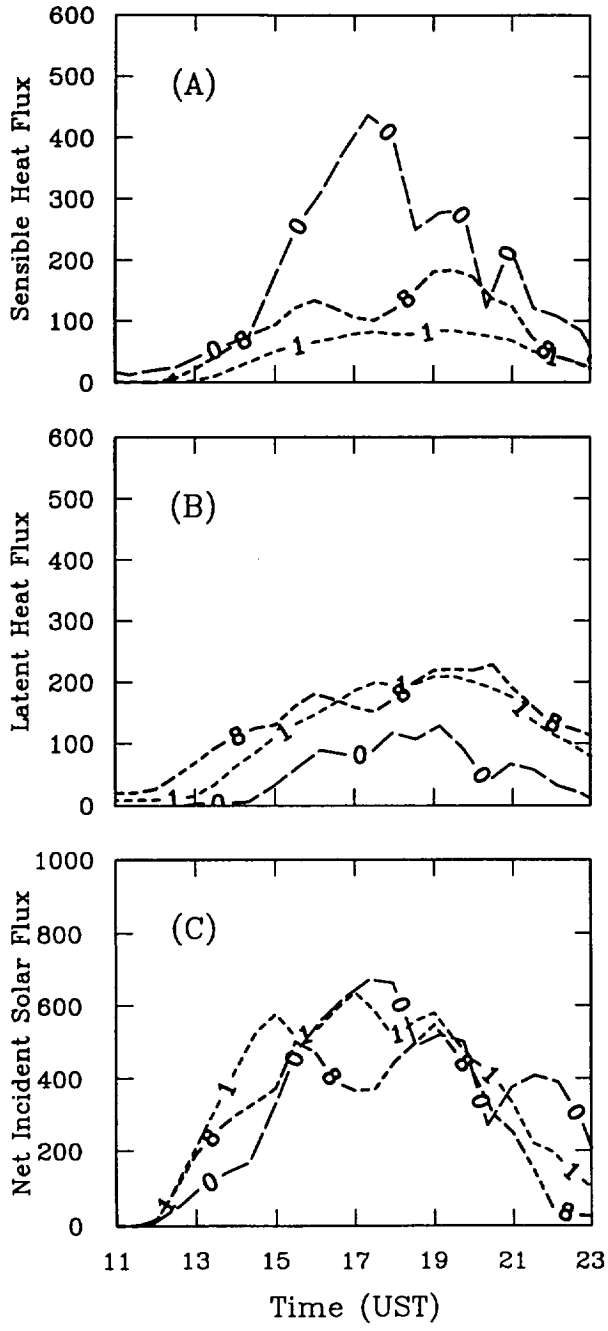
(A)
Sensible Heat Flux
600
500
400
300
200
100
0
(B)
Latent Heat Flux
600
500
400
300
200
100
0
(C)
Net Incident Solar Flux
1000
800
600
400
200
0
11
13
15
17
19
21
23
Time (UST)

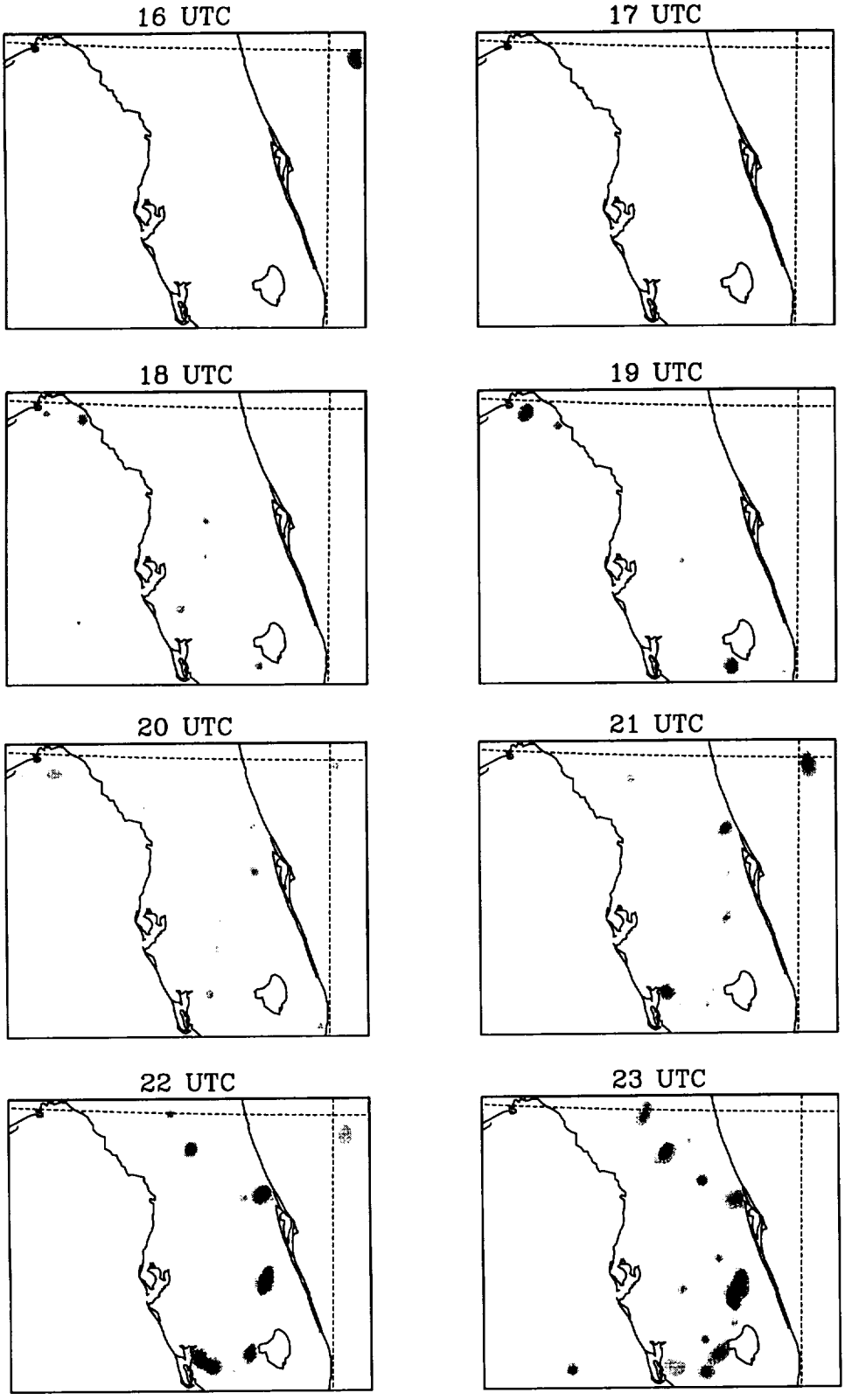
16 UTC
17 UTC
18 UTC
19 UTC
20 UTC
21 UTC
22 UTC
23 UTC
0
0.1
1
2
3
4
5
6
7
Cloud Condensate (g/kg)

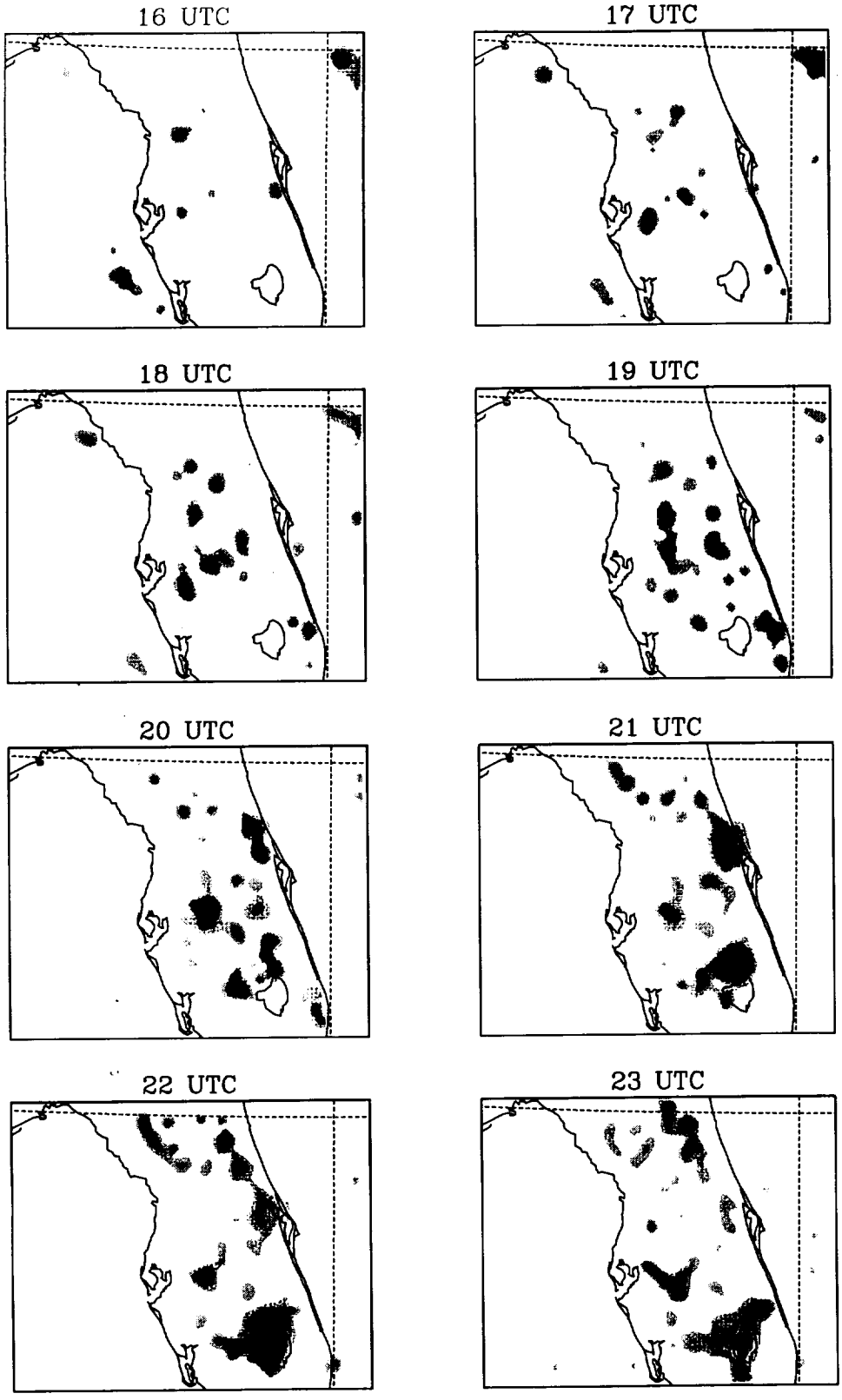
16 UTC
17 UTC
18 UTC
19 UTC
20 UTC
21 UTC
22 UTC
23 UTC
0
0.1
1
2
3
4
5
6
7
Cloud Condensate (g/kg)

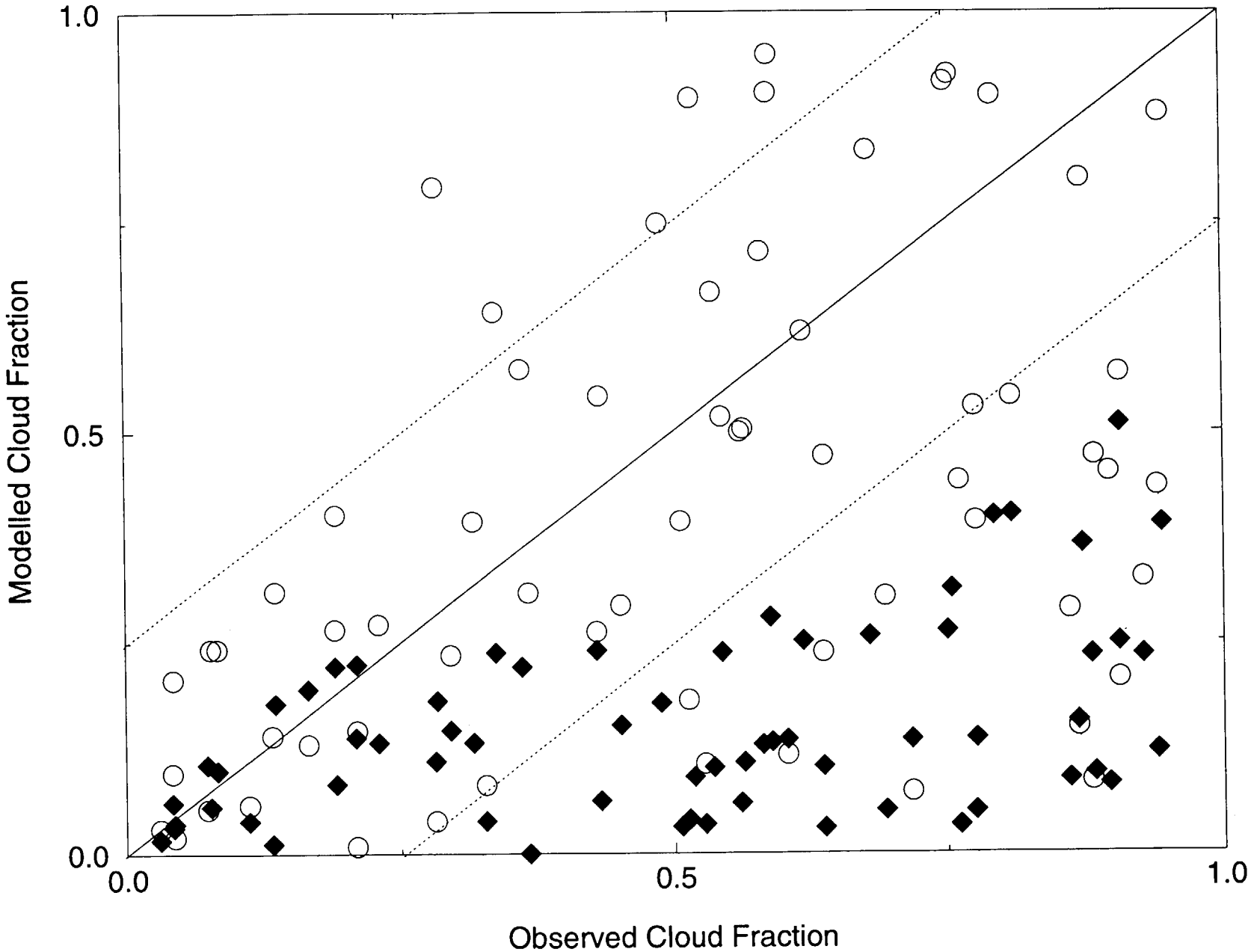
1.0
0.5
0.0
0.0
0.5
1.0
Modelled Cloud Fraction
Observed Cloud Fraction

No Modification (Factor 0)

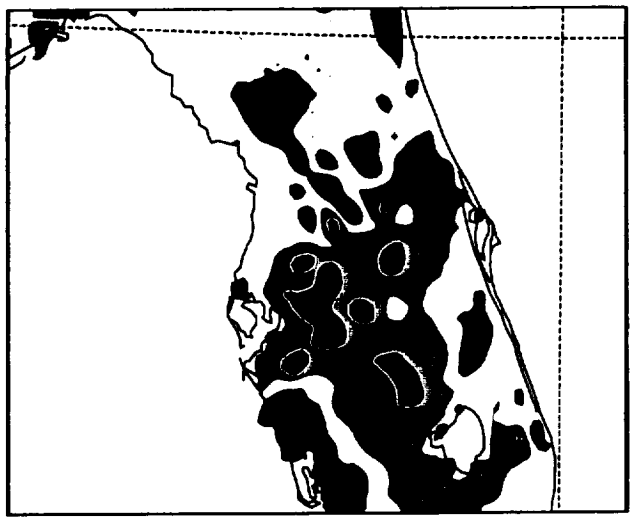

Contribution From Factor 1

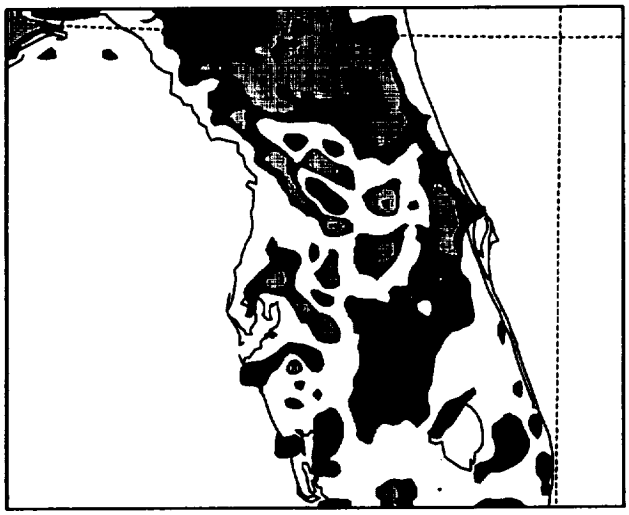

Contribution From Factor 2

Joint Contribution From Factors 1 and 2

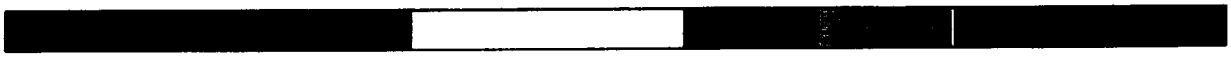

−3 −2 −1 −0.5 0 0.5 1 2 3 4

Potential Temperature Perturbations (K)

No Modification (Factor 0)

Cont. From Factor 1

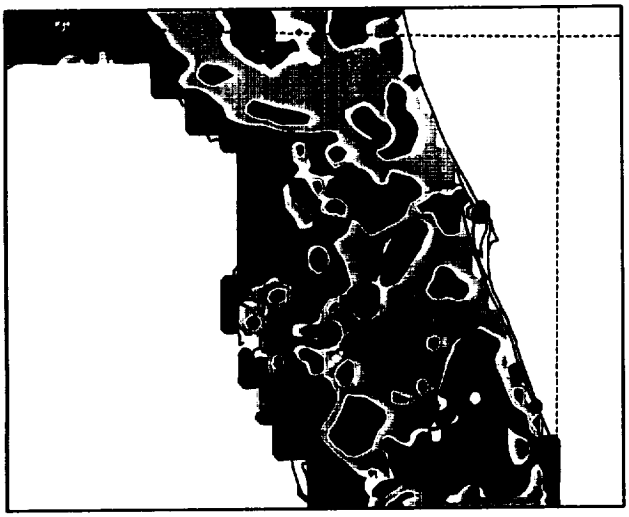

Cont. From Factor 2

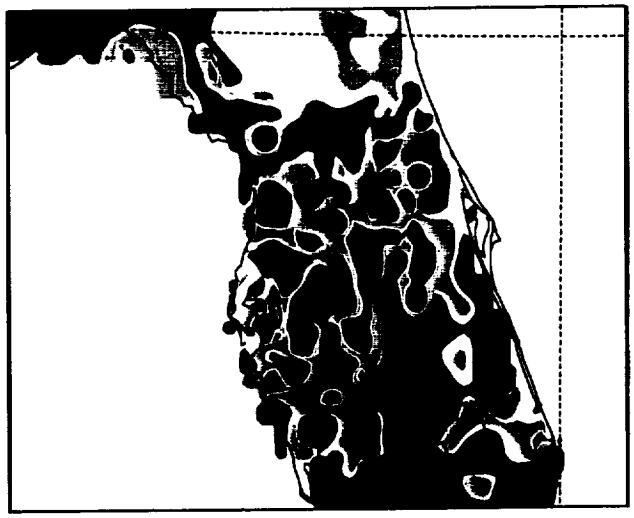

Cont. From Factor 3

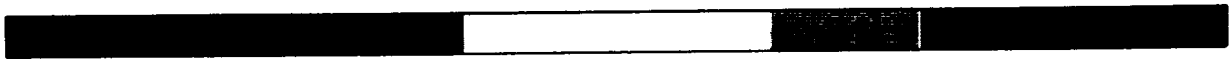

−10 −7 −4 −1 0 1 15 30 50

Relative Humidity Perturbations (%)

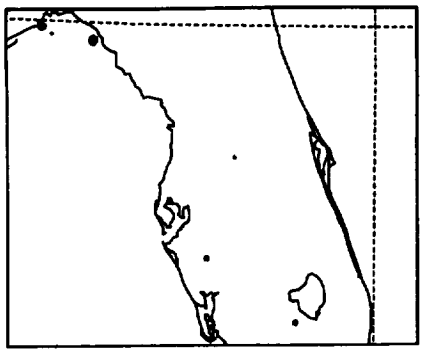

No Modification (Factor 0)

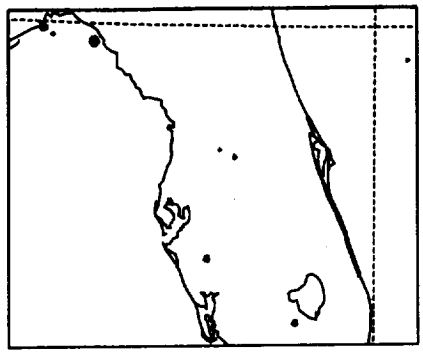

Cont. From Factor 1

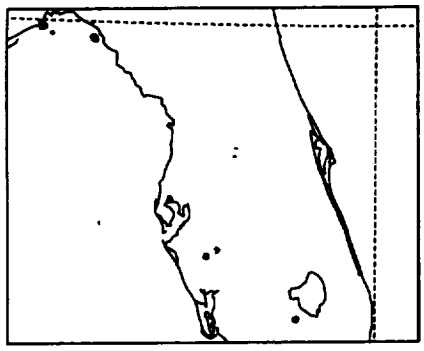

Cont. From Factor 2

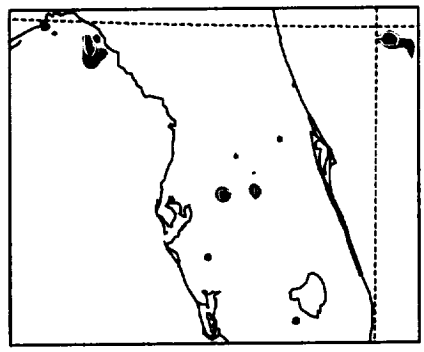

Cont. From Factor 3

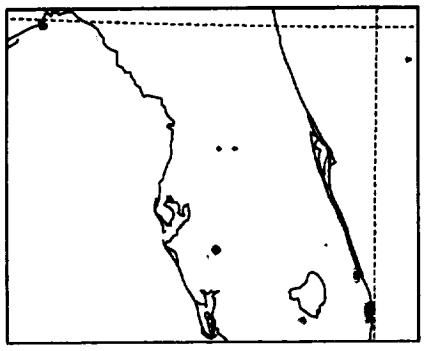

J.–C. Factors 1 and 2

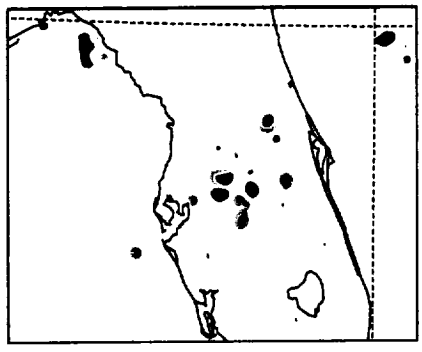

J.–C. Factors 1 and 3

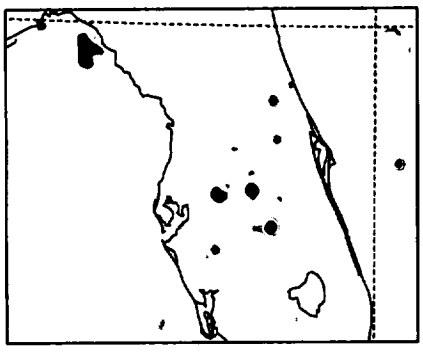

J.–C. Factors 2 and 3

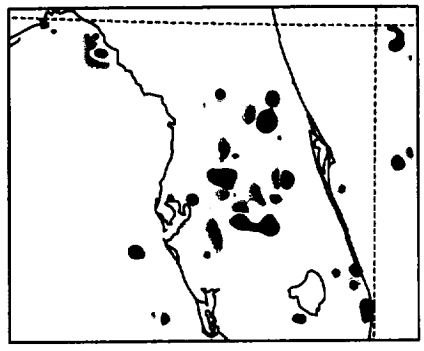

S.–C. Factors 1, 2, and 3

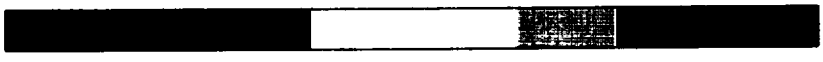

−7 −5 −3 −1 0 1 3 5 7

Cloud Condensate (g/kg)